

Long-term Variations in Albedo, Solar Flux, and Climatic Parameters in Burkina Faso (1984-2022)

Abstract

In this work, we examined the effects of albedo and solar flux on climate parameters in Burkina Faso (1984-2022). We found that albedo amplitudes in Dori region are higher than those in Ouagadougou, and those in Ouagadougou are higher than those in Bobo Dioulasso. We also observed a continuous decrease in albedo, leading to an increase in temperature, humidity, and precipitation. These climatic conditions may increase the risks of prolonged droughts and floods. This drop in albedo is linked to solar activity, growing urbanization, deforestation and global climate change. Low solar activity and solar high-speed flows caused by regions of corotative interactions lead to heavy precipitation. Low solar activity and solar high speed flows caused by corotative interactions regions lead to heavy precipitation. The use of reflective construction materials, i.e. high albedo, in urban infrastructure and stopping the transformation of forests into cultivable land can contribute to mitigating the diminution in albedo and consequently global warming.

Keywords : Albedo, Solar flux, Temperature, Precipitation, Solar Activity, Climate, Burkina Faso

1. Introduction

The Sun is the main source of energy, through its electromagnetic radiation which heats the earth's atmosphere and determines meteorological processes. Albedo is the ability of surfaces to reflect sunlight (heat from the sun). Measured on a scale of 0 to 1; an albedo value of 0 indicates that all light is absorbed by the surface (dark surfaces) and is not reflected and a value of 1 indicates that all light is reflected by the surface (Clear surfaces) and there is no absorption. Although only one of many factors contributing to climate change, surface albedo is an important parameter in the energy balance of the land cover and is considered an essential climate variable. Variations in surface albedo can be used as a diagnostic tool for local climate change according to authors such as [1]; [2]. Climate change is defined as general changes in climate over time. This includes global warming, more frequent and intense extreme weather events (like hurricanes and monsoons), and bizarre weather conditions. A change in albedo or a change in global temperatures can create a feedback loop between the two. The Earth's albedo has been declining for decades, contributing to global warming. Local/regional climate change caused by deforestation and land use changes is synergistic with global warming, causing a more dynamic climate change process [3]. The temporal and spatial variation of albedo has been closely related to global climate change as well as regional weather and environment [4]; [5]. [6] found a strong inverse exponential relationship with a correlation ($r = 0.95$) between satellite-observed albedo and precipitation. Similar relationships have been discovered in West Africa between albedo and precipitation by several researchers [7]; [8]; [9]. [10] showed the existence of a negative correlation between albedo and land surface temperature, with $R^2 = -0.6109$. [11] Showed that albedo influences surface temperature. [12] showed that higher rainfall is associated with lower albedos. [13] Showed that flooding caused by heavy precipitation in Canada tends to follow the arrival

38 of high-speed solar wind streams from coronal holes. [14]revealed that an active Sun is associated
39 with clear skies, while a quiet Sun is associated with cloudy skies, leading to more precipitation and
40 cooling of the Earth's atmosphere.(Feynman & Ruzmaikin, 1999); (Carslaw et al., 2002) and
41 (Yeghikyan, 2020) have also shown that cosmic rays, which are high-energy particles originating from
42 outside our solar system, can influence the formation of clouds, which generally have a high
43 albedo.The objective of this work is to analyze the long-term variations of albedo, solar flux and climatic
44 parameters in Burkina Faso (1984-2022). For our study, we chose three areas of Burkina Faso with different
45 vegetation covers (Fig.1).The Sahelian zone in the north with precipitation less than 600 millimeters per
46 year (mm/year), the Sudano-Sahelian region on a savannah plateau with precipitation of 600 to 900
47 millimeters per year (mm/year) and slightly cooler temperatures, and the wetter southern Sudanian
48 zone with average precipitation between 900 and 1,200 mm/year.

49

50 **2. Data and Methodology**

51 In this work, we used annual averages of albedo, precipitation, temperature and specific humidity,
52 available at [43]. The solar wind speed available on the site [44] was used to calculate the solar wind
53 energy flux ($\text{kg}\cdot\text{s}^{-3}$)using the formula:

$$54 \quad E_{sw} = \frac{1}{2} \rho_{sw} V_{sw}^3$$

55 $\rho_{sw} = 1408 \text{ kg/m}^3$ and represents the density of the solar wind.We have also used the sunspot number
56 available on the site [45]. Hourly cosmic ray data were obtained from the Thule Neutron Monitoring
57 Station (76.5°N, 68.5°W, 26.0 m) with a geomagnetic cut-off rigidity of 1.0 GV. Then we calculated the
58 annual averages of cosmic raysto see their influence on albedo and climatic parameters.

59 These data were used to analyze the impact of albedo and solar flux on climate parameters in three
60 cities in Burkina Faso, namely Bobo-Dioulasso (latitude=11.149; longitude=-4.242), Ouagadougou
61 (latitude=12.365; longitude=-1.507) and Dori (latitude=14.007; longitude=-0.073). These three cities
62 are located in different climatic zones (figure 1) of Burkina Faso.



Figure 1: Climatic zones of Burkina Faso

3. Results and discussion

From figures 2 to 7, the relationship between albedo, solar flux and climatic parameters in Burkina Faso is investigated for the period 1984-2022.

Figure 2, presents the precipitation and albedo profiles in three cities Bobo Dioulasso, Ouagadougou and Dori during the period 1984 to 2022. In Figure 2.a, we observe a decrease in surface albedo from 1984 to 1990. During this period, we recorded a drop in precipitation. From 1990 to 1999 we observe a constant evolution of the albedo then a slight increase in the albedo. During this period, we observe a fluctuation in precipitation, but we can notice an increase in maximum amplitudes. During the period 2000 to 2001, a strong decrease in albedo is observed. The albedo drops from 0.2 to 0.16. Then we observe a strong fluctuation and continuous decrease in albedo until 2022. During this period we also record a strong fluctuation in precipitation; but we can also notice a continuous increase in the maximum amplitudes of precipitation. The highest rainfall is recorded in 1998 (1223.44 mm), 2010 (1244.53 mm) 2019 (1455.47 mm) and 2021 (1288 mm).

In Figure 2.b, we observe a decrease in albedo from 1984 to 1989 and a stable evolution of maxima amplitude of the precipitation. A fluctuation in albedo is observed from 1989 to 2000 with an increase in maximum precipitation amplitudes. From 2000 to 2001 a sudden decrease in albedo is observed and a drop in precipitation is also observed. From 2001 until 2022, a linear and constant evolution of the albedo is observed, except 2012 and 2021 which records a slight fluctuation. The year 2021 records the lowest albedo during our study period. During the period 2001 to 2022, a strong fluctuation in precipitation is observed; but overall we remark an increase in the maximum amplitudes of precipitations. The lowest precipitation was observed in 1987 (305.86 mm) and 1990 (295.31 mm).

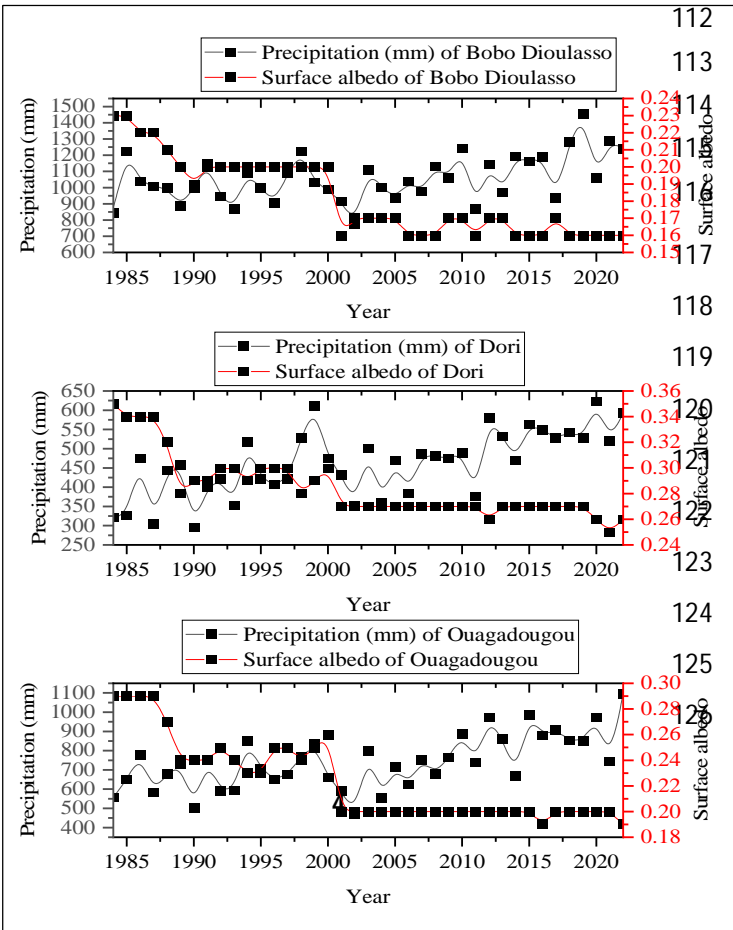
In Figure 2.c, we observe a constant evolution of the albedo from 1984 to 1987 before gradually decreasing from 1987 to 1989. During this period we observe a decrease in the maximum amplitudes of precipitations. From 1989 to 2000 we observe a strong fluctuation in albedo. During this period an

89 increase in maximum precipitation is observed. From 2000 to 2001, the albedo drops sharply, leading
 90 to a sudden decrease in precipitation until 2002. Then from 2001 to 2022, a linear and constant
 91 evolution of the albedo is observed with slight variations in 2016 and 2022. During this period there is
 92 a strong fluctuation in precipitation with an increase in maximum amplitudes. The lowest precipitation
 93 is recorded in 1983 (442.97 mm), 1990 (500.98 mm) and 2002 (469.34 mm) and the highest
 94 precipitation is recorded in 2012 (970.31 mm), in 2015 (986.13 mm), 2020 (970.31 mm) and 2022
 95 (1096.92 mm)

96 Figure 3, presents the temperature and albedo profiles of Bobo Dioulasso, Ouagadougou and Dori
 97 during the period 1984 to 2022. In Figure 3.a, we observe a decrease in albedo from 1984 to 1990;
 98 from 1991 to 2000 a linear and constant evolution of the albedo is observed. During these periods we
 99 observe a decrease in the earth's temperature from 1984 to 1985 then increases slightly from 1985 to
 100 1987 before fluctuating slightly around 27°C to 28°C from 1987 to 2000. Then the albedo drops sharply
 101 from 2000 to 2001. During this period the temperature increased sharply and recorded the highest
 102 temperature in 2002 (29.06 °C) during our study period. Then a slight fluctuation in albedo followed by
 103 a weak fluctuation in temperature around 27°C to 28°C. The lowest temperature was recorded in 1986
 104 (26.63°C).

105 In Figure 3.b, we observe a continuous decrease in the albedo from 1984 to 1989. During this period,
 106 we observe an increase in temperature with a peak in 1987 (30.01 °C) before decreasing until 'in
 107 1989. From 1989 to 2000 we observe a weak fluctuation in the albedo and during this period, the
 108 largest peak in temperature is observed in 1990 (30.3 °C) before gradually decreasing until 1999.
 109 From 2000 the albedo drops sharply until 2001, then a linear and constant evolution is observed until
 110 2022, with slight fluctuations in 2012 and 2021. During this period heat waves are observed, with the

111 largest heat
 112 peak
 113 recorded in
 114 2004 (30.42
 115 °C).



a

b

c

127

128

129

130

Figure 2: Precipitation and albedo profile during the period 1984-2022

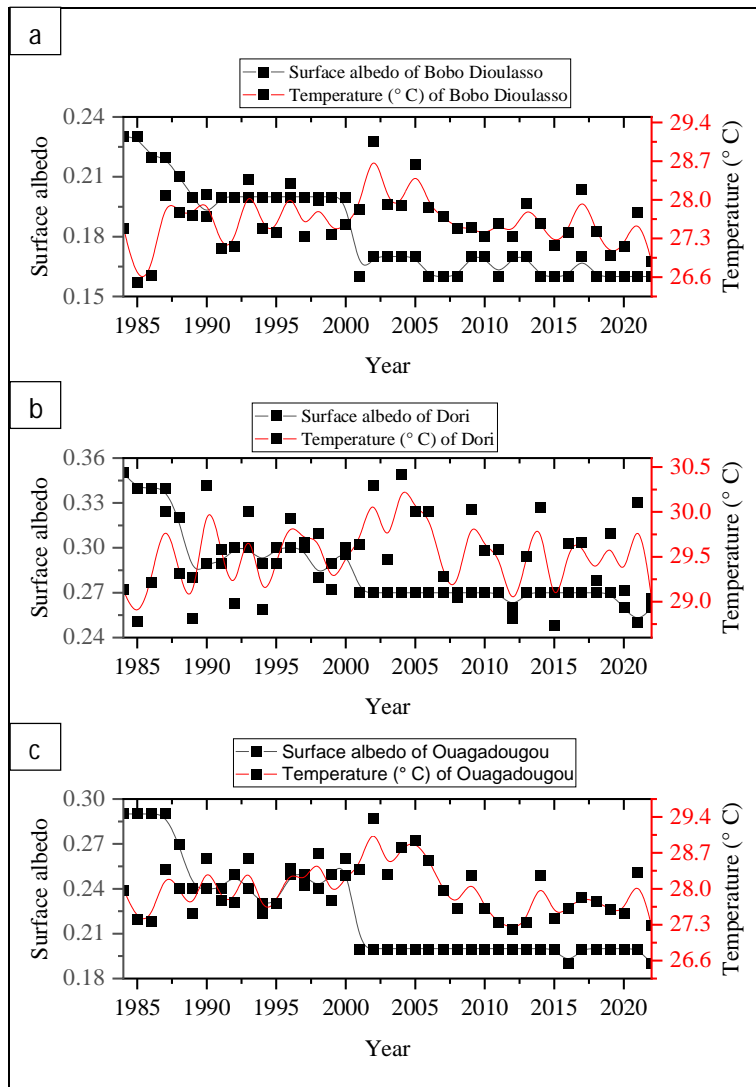
131

In Figure 3.c, we observe a linear and constant evolution of the albedo from 1984 to 1987. During this period a decrease in temperature is observed from 1984 to 1986. A decrease in the albedo is observed from 1987 to 1989 and an albedo fluctuation around 0.23 to 0.26 from 1990 to 2000. During these periods, a weak temperature fluctuation around 27 °C and 28 °C is observed. A sudden decrease in albedo was recorded from 2000 to 2001 and led to a sharp increase in temperature. The highest temperature was recorded in 2002 (29.37°C) during our period covered by our study.

137

Figure 4, presents the temporal evolution curves of the annual averages of precipitation and specific humidity in the cities of Bobo Dioulasso, Ouagadougou and Dori during the period 1984 to 2022. The specific humidity (absolute) is the actual amount of moisture in the form of water vapor in the air. Specific humidity is measured in grams of water vapor per kilogram of air (g/kg). The two parameters studied present a good correlation. The correlation is 0.72 for the city of Bobo Dioulasso, 0.76 for the city of Ouagadougou and 0.69 for the city of Dori. The highest precipitation coincides with the highest specific humidity. Also the lowest precipitation coincides with the lowest specific humidity. We also observe an increase in the maximum amplitudes of precipitation and specific humidity from 2001 to 2022. In Figure 4.a, the lowest specific humidity and the lowest precipitation is recorded in 2002 (11.11 g/kg; 775.52mm). The highest specific humidity and precipitation are recorded in 2010 (13.37 g/kg; 1244.53 mm) and in 2019 (13.12 g/kg; 1455.47 mm). In Figure 4.b, the lowest specific humidity is recorded in 1984 (8.42 g/kg), in 1987 (8.36 g/kg), in 2000 (8.54 g/kg) and in 2001 (8.48 g/kg) and the lowest precipitation is observed in 1987 (305.86 mm) and 1990 (295.31 mm). The highest specific humidity was observed in 2010 (10.31 g/kg), in 2012 (10.5 g/kg) and the highest precipitation was recorded in 1999 (611.72 mm), in 2012 (580 .08 mm) in 2015 (564.26 mm) and 2020 (622.27 mm). In Figure 4.c, the lowest specific humidity and precipitation are observed in 1983 (9.64 g/kg; 442.97 mm) and in 2002 (9.64 g/kg; 469.34 mm). High specific humidity and precipitation are observed in 2010 (12.15 g/kg; 885.94 mm) in 2012 (12.08 g/kg; 970.31 mm) in 2022 (11.84 g/kg; 1096. 92mm). These observations show that high specific humidity leads to heavy precipitation.

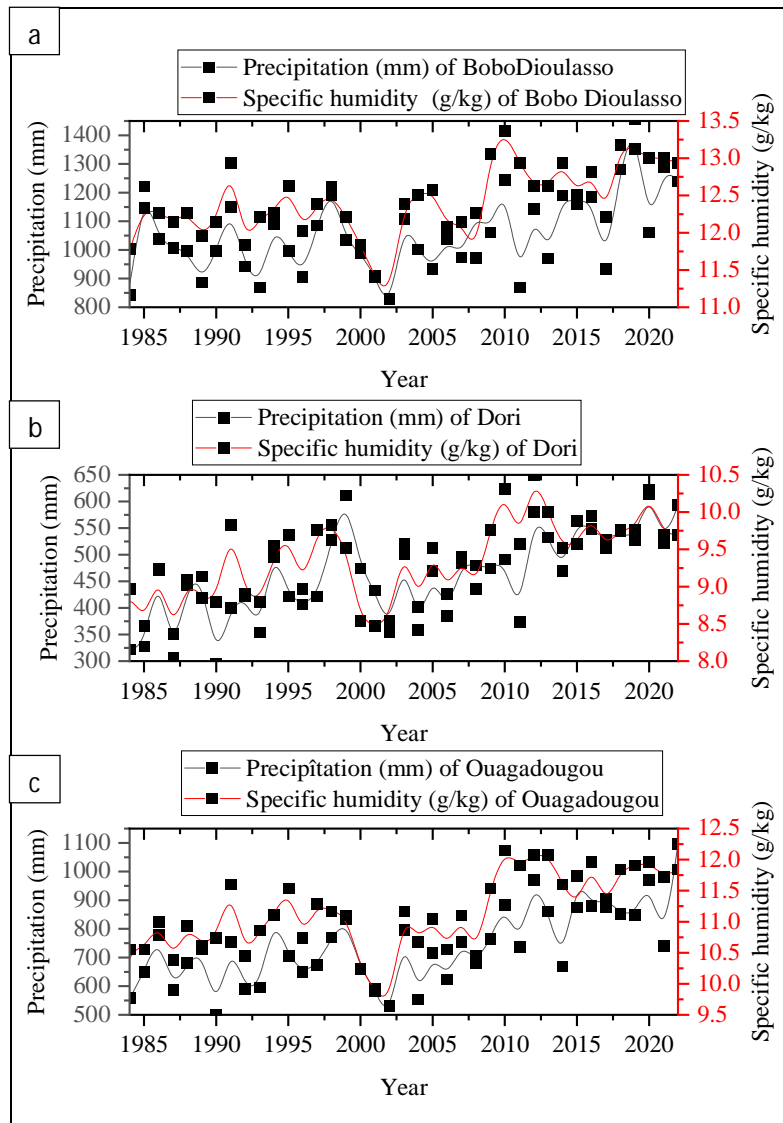
155



156

157

Figure 3: Surface temperature and albedo profile during the period 1984-2022



158

159

Figure 4: Profile of precipitation and specific humidity during the period 1984-2022.

160

Through the analysis of figures 2, 3 and 4 we can see that the quantity of precipitation varies greatly

161

depending on the specific humidity, which varies with the temperature. Indeed, as the temperature

162

increases, the air is able to retain more and more humidity. We are more likely to receive rain when

163

humidity is higher because water vapor expands more quickly. This is based on the Clausius-

164

Clapeyron (CC) relationship which states that as temperature increases, the atmosphere has the

165

capacity to retain more moisture, at a rate of 6% to 7% °C⁻¹ [18]. Thus, extreme precipitation scales

166

with surface water or the water column [19],[20], so we can expect extreme precipitation to increase

167

with temperature increase. We also observed that a continued decrease in albedo leads to heat

168

waves. Indeed, the reduction in albedo leads to an increase in the absorption of solar radiation by the

169

ground and therefore the transfer of sensible and latent heat to the atmosphere. This produces higher

170

global warming. These observations are in agreement with the work of [10] which showed the

171

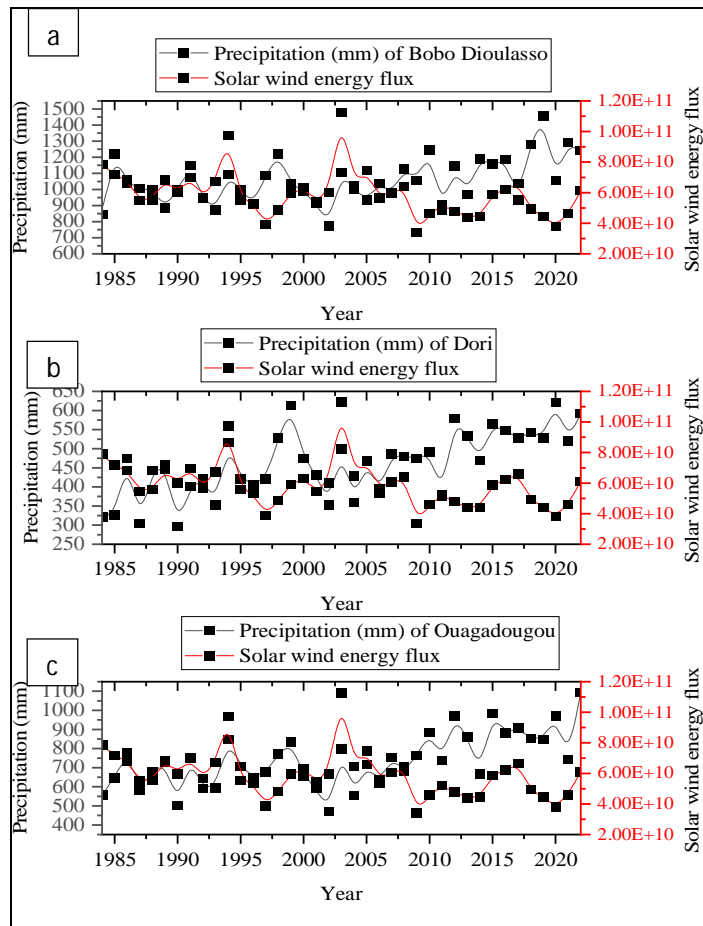
existence of a negative correlation between albedo and land surface temperature, with $R^2 = -0.6109$.

172

Also, [11] showed that albedo influences surface temperature. The decrease in albedo contributes to

173 the increase in convective clouds, and therefore precipitation. This global warming and increased
174 precipitation causes the evaporation of a greater quantity of water, therefore high specific humidity,
175 which can lead to more intense droughts and a higher risk of flooding. Overall, weird weather
176 conditions. These observations show that a change in albedo influences climatic parameters
177 (temperature, specific humidity and precipitation). These observations are in agreement with the work
178 of [12] who found higher rainfall at lower albedos. We also note that the amplitude of precipitation
179 and specific humidity is important in Bobo Dioulasso compared to Ouagadougou and similarly the
180 amplitude of precipitation and specific humidity is important in Ouagadougou compared to Dori. The
181 amplitude of temperature and albedo are significant in the town of Dori compared to Ouagadougou
182 and Ouagadougou compared to Bobo-Dioulasso. **This is explained by the fact that the soils of Dori and
183 Ouagadougou are sandy and dry (light surfaces), unlike the soil of Bobo Dioulasso which is a crop soil
184 (dark surface).** However, a continuous decrease in albedo is observed in all three cities. This is
185 explained on the one hand by the difference in plant cover and the quantity of water in the soil in these
186 different zones. On the other hand, Burkina Faso knows an increase in population in recent decades
187 as well as rapid urbanization and industrialization concentrated in large cities. This caused a great
188 revolution in land use. This revolution is accompanied by a significant thermal change, creating a
189 thermal imbalance between urban and rural areas. **Indeed according to the work of (Zutao Ouyang et
190 al 2022) who, through an empirical approach to the climatic effects of urbanization, found a decrease
191 in albedo due to urbanization.** This series of extreme heat waves increases cooling energy
192 consumption in buildings, deteriorates air quality and affects people's health [21], leading to an
193 increase in health and mortality [22];[23],[24];[25]. Possible symptoms caused by heat stress include
194 swelling, rashes, and heat stroke related to neurological disorders when body temperature reaches
195 40.6°C [26]. Thus, strategies must be implemented to reduce the conditions of global warming in
196 Burkina Faso. Several studies have shown a direct link between high urban temperatures and the lack
197 of vegetation, highlighting the potential of vegetation to reduce extreme temperatures, especially
198 during the hot season, through two effects: evapotranspiration and shading [27];[28]. Deforestation
199 can decrease evapotranspiration and increase surface temperatures by 3° to 5°C [29].[30] through
200 deforestation simulation studies have shown either a decrease in precipitation due to the weakening of
201 precipitation recycling, or an increase in precipitation due to the intensification of convection over
202 areas heterogeneity of the earth's surface. For [31], urbanization can potentially have a global
203 warming effect by reducing the Earth's albedo. Tropical forests are increasingly recognized as major
204 resources for mitigating climate change [32]. The work of [2] showed that reducing deforestation of all
205 forest types, converting annual or grassland agriculture to perennial agriculture, and properly selecting
206 greenhouse covers for new protected agricultural systems could help mitigate climate change
207 regional. According to the work of [10]; [31], green roofs have a higher albedo than many conventional
208 black/brown roofs. The albedo of urban land is 0.01–0.02 lower than that of adjacent cultivated land
209 [33]. **This low albedo observed in urban areas is due to the predominance of dark materials such as
210 asphalt and concrete, which absorb a lot of heat. This contributes to a significant rise in temperatures
211 more in cities than in rural areas.** The albedo of urban land can be regulated and improved by using
212 more reflective materials and also by reducing deforestation.

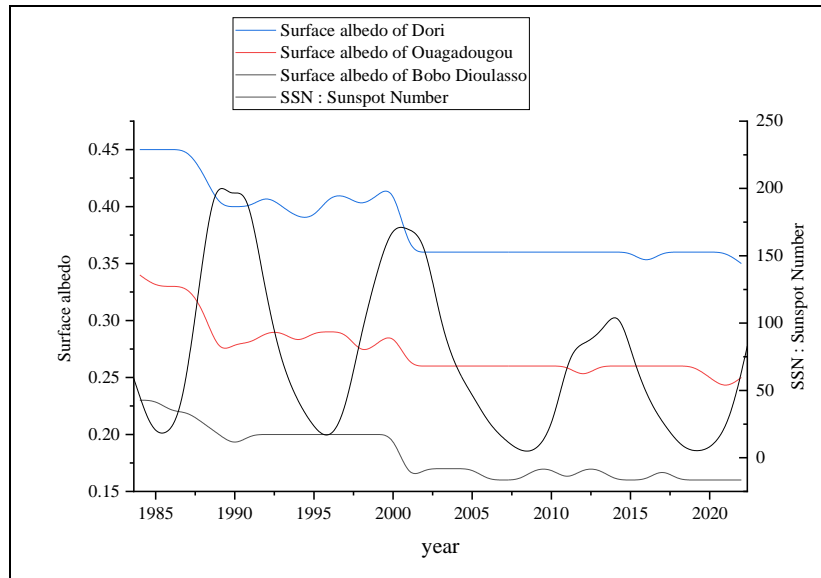
213 Figure 5 presents the profile of the solar wind energy flux and precipitation of Bobo-Dioulasso,
214 Ouagadougou and Dori during the period 1984 to 2022. In Figures 5.a, 5.b and 5.c, the two
215 parameters studied present a weak correlation. However, we can observe some peaks in the solar
216 wind energy flux to coincide with heavy annual precipitation. This can be clearly observed in 1994 and
217 2003 which correspond to periods of the descending phases of solar cycles 22 and 23. Heavy
218 precipitation is also observed when weak solar wind energy flux are recorded. These periods coincide
219 with the solar minimum of solar cycles, which are dominated by slow solar winds [31], [32].
220 Exceptionally, we generally observe a drop in the amplitude of the solar wind energy flux after the long
221 solar minimum which preceded solar cycle 23 (2008-2022). During this period, there is an increase in
222 precipitation. These observations are in agreement with the work of [14] who found that precipitation is
223 important at solar minimum where quiet activity is dominant. According to the work of [36],[37], solar
224 cycle 24 at has knows a lower solar activity compared to solar cycle 23. Also, according to the work of
225 [13], which, analyzing the storm of December 5 and 6, 2010 in New Brunswick found heavy
226 precipitation and a storm surge that caused flooding. This coincided with the arrival of a high-speed
227 HSS/CIR flow with dense high-density plasma at its leading edge on 6 December. According to the
228 work of [38],[39], CIRs play a dominant role as a source of geomagnetic disturbances during the solar
229 minimum. Indeed, as the Sun rotates, high-speed fluxes (HSS) emitted from coronal holes can interact
230 with ambient slow solar wind fluxes, compressing the plasma at the boundary, increasing the density
231 in the region of slow solar wind. If the configuration of the solar corona is stable, the pattern of
232 interaction regions repeats with each rotation of the Sun, and they are called corotating interaction
233 regions [40],[41]. In the fast solar wind, the kinetic energy of the plasma is converted into thermal
234 energy, resulting in heating of the plasma and a decrease in density [41]. During this interaction of fast
235 solar winds and slow solar winds the plasma becomes very dense and very hot and contributes to
236 heating the convective clouds, increasing precipitation. We can therefore say that solar activity is one
237 of the many factors that affect climatic conditions, in particular precipitation.



238

239 Figure 5: Profile of precipitation and the solar wind energy flux during the period 1984 to 2022.

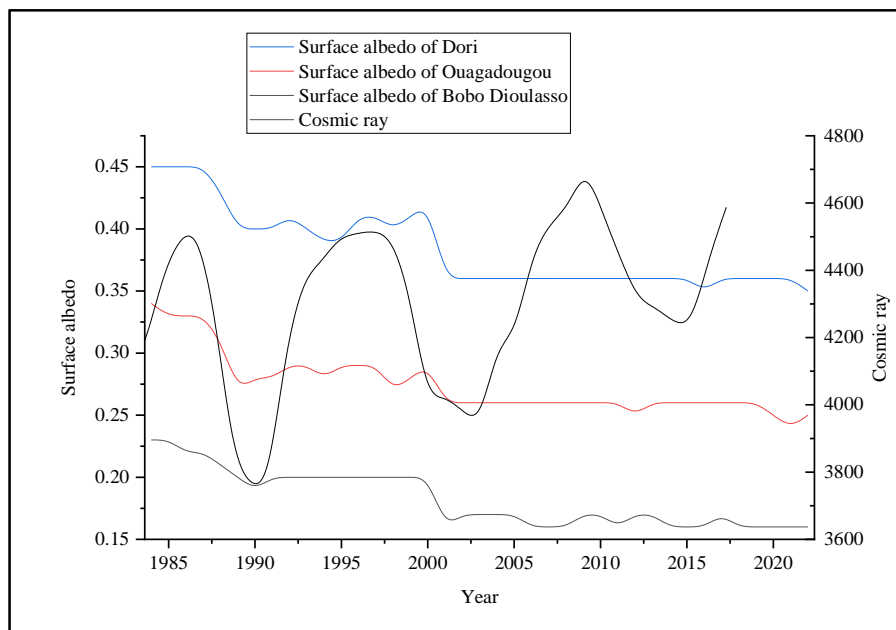
240 Figure 6, presents the temporal evolution profiles of the sunspot number and the surface albedo of
 241 Bobo Dioulasso, Ouagadougou and Dori during the period 1984 to 2022. The two parameters studied
 242 present a weak correlation. However, we can notice that the abrupt decreases in albedo are observed
 243 at the maximum phase of each solar cycle. We also observe a constant evolution of the albedo after
 244 the solar minimum of solar cycle 23, with slight fluctuations in 2011 and 2017 in Bobo-Dioulasso, in
 245 2016 in Ouagadougou and in 2012 and 2021 in Dori. According to [42], the Sun is, on average, more
 246 irradiating at maximum activity than at a minimum of its cycle activity approximately 11 years. Also
 247 according to [43], the variation in magnetic activity during the course of the 11-year cycle influences
 248 not only the sunspot number and the magnetic flux but also the radiation emitted by the Sun and
 249 which we receive on Earth called total or “constant” solar irradiance. [44] showed that the total
 250 irradiance varies in phase with the solar cycle by about 0.1%: the higher the sunspot number, the
 251 higher the flux we receive from the Sun, due to of the massive presence of faculae which are brighter
 252 zones. Furthermore, during the solar maximum, coronal mass ejections are the most important events
 253 and dissipate a large amount of energy in the interplanetary medium [14]. Thus, we can say that the
 254 Earth receives a large amount of energy during the solar maximum compared to other phases of the
 255 solar cycle. This can lead to a reduction in surface albedo. This is clearly observed in 1989 and 1990 at
 256 solar cycle 22 and in 2001 at solar cycle 23, where a sudden decrease in albedo was recorded.



257

258 Figure 6: Profiles of the sunspot number and the surface albedo during the period 1984-2022.

259 Figure 7, presents the cosmic ray and albedo profiles of Bobo-Dioulasso, Ouagadougou and Dori
 260 during the period 1984 to 2022. The two profiles show a weak correlation, but however the lowest
 261 cosmic ray values are accompanied by a sudden decrease in albedo. We can also note that the
 262 amplitudes of cosmic rays are significant over the last decade (2005-2022), with an almost linear
 263 evolution of the albedo. This is explained by the low solar activity observed during this period.
 264 According to the work of [36];[37]), the solar activity of solar cycle 24 has been weak compared to
 265 solar cycle 23, and is also manifested in the solar magnetic field. Furthermore, according to the same
 266 authors, the calm Sun causes significant cloud cover while the active Sun induces less cloud cover.
 267 [45] claims that the magnetic field of the solar wind influences the cosmic rays responsible for the
 268 formation of clouds.



269

270 Figure 7: Cosmic ray and surface albedo profiles during the period 1984-2022.

271 Thus, the solar minimum going hand in hand with an increase in cosmic radiation received by the
272 Earth, condensation would be made more efficient and the increase in cloud cover would be favored.
273 Thus we can say that intense solar activity releases a large quantity of energy onto Earth and a low
274 rate of cosmic rays. Which leads to a drop in albedo, low cloud cover, and fluctuating temperatures.
275 Low solar activity leads to a high rate of cosmic rays in the interplanetary medium and this leads to
276 significant cloud cover. Low solar activity results in a high rate of cosmic rays (Figure 7) and a lower
277 amount of solar flux (Figure 6) in the interplanetary medium and this results in significant cloud
278 cover. Thus part of the solar energy would be absorbed by this cloud cover, and would have less
279 impact on the surface albedo.

280 4. Conclusion

281 In this study, we examined solar flux and climatic parameters in three cities in Burkina Faso, located in
282 three different climatic zones. The albedo amplitudes of Dori are higher than those of Ouagadougou
283 and those of Ouagadougou higher than those of Bobo Dioulasso. This study reveals a continued
284 decrease in albedo in Burkina Faso leading to significant global warming. This global warming causes
285 an increase in temperature, specific humidity and precipitation, increasing the risks of severe droughts
286 and floods. This decline in albedo can be explained by increasing urbanization, deforestation,
287 manifestations of solar activity and global climate change. Heavy precipitation is observed during
288 periods of low solar activity and also during high-speed flow events caused by regions of co-rotating
289 interactions. The continued decrease in albedo can be mitigated by favoring more reflective
290 construction materials, i.e. high albedo, and stopping the transformation of forests into cultivatable
291 land. A small-scale study and extension to other regions could help to better understand the impact of
292 solar activity on albedo and its influence on climate parameters.

293

294 Acknowledgment

295 The authors would like to thank the reviewers for their detailed and insightful comments and
296 constructive suggestions. Special thanks to all providers of data used. The solar wind data are
297 available at: <https://omniweb.gsfc.nasa.gov/form/dx1.html>; the sunspot number data are available at:
298 <http://www.sidc.be/silso/>; the climatic parameters data (Albedo, Precipitation, Specific Humidity and
299 Temperature) are available at: <https://power.larc.nasa.gov/data-access-viewer/>; the cosmic ray data
300 are available at Thule Neutron Monitoring Station.

301 Conflicts of Interest

302 The authors have not declared any conflicts of interests.

303 References

- 304 1. Guo, T., He, T., Liang, S., Roujean, J.-L., Zhou, Y., Huang, X., 2022. Multi-decadal analysis of high-
305 resolution albedo changes induced by urbanization over contrasted Chinese cities based on
306 Landsat data. *Remote Sens. Environ.* 269, 112832. <https://doi.org/10.1016/j.rse.2021.112832>
- 307 2. Santos Orozco, D.L., Ruiz Corral, J.A., Villavicencio García, R.F., Rodríguez Moreno, V.M., 2023.
308 Deforestation and Its Effect on Surface Albedo and Weather Patterns. *Sustainability* 15,
309 11531. <https://doi.org/10.3390/su151511531>
- 310 3. Hu, Y., Hou, M., Zhao, C., Zhen, X., Yao, L., Xu, Y., 2019. Human-induced changes of surface
311 albedo in Northern China from 1992-2012. *Int. J. Appl. Earth Obs. Geoinformation* 79, 184–191.
312 <https://doi.org/10.1016/j.jag.2019.03.018>
- 313 4. He, T., Wang, D., Qu, Y., 2018. Land Surface Albedo. In S. Liang (Ed.), *Comprehensive Remote*
314 *Sensing. Volume 5: Earth's Energy Budget* (pp. 140-162). Amsterdam: Elsevier.
315 <https://doi.org/10.1016/B978-0-12-409548-9.10370-7>
- 316 5. Zhao, F., Lan, X., Li, W., Zhu, W., Li, T., 2021. Influence of Land Use Change on the Surface
317 Albedo and Climate Change in the Qinling-Daba Mountains. *Sustainability* 13, 10153.
318 <https://doi.org/10.3390/su131810153>
- 319 6. Bhattacharya, B., Gunjal, K., Panigrahy, S., Parihar, J., 2011. Albedo-rainfall Feedback Over Indian
320 Monsoon Region Using Long Term Observations Between 1981 to 2000. *J. Indian Soc. Remote Sens.*
321 39, 393–406. <https://doi.org/10.1007/s12524-011-0136-9>
- 322 7. Charney, J., Quirk, W., Chow, S., Kornfield, J., 1977. A Comparative Study of the Effects of Albedo
323 Change on Drought in Semi-Arid Regions. *J. Atmospheric Sci.* 34.
324 [https://doi.org/10.1175/1520-0469\(1977\)034<1366:ACSOTE>2.0.CO;2](https://doi.org/10.1175/1520-0469(1977)034<1366:ACSOTE>2.0.CO;2)
- 325 8. Fuller, D.O., Ottke, C., 2002. Land Cover, Rainfall and Land-Surface Albedo in West Africa. *Clim.*
326 *Change* 54, 181–204. <https://doi.org/10.1023/A:1015730900622>
- 327 9. Govaerts, Y., Lattanzio, A., 2008. Estimation of surface albedo increase during the eighties Sahel
328 drought from Meteosat observations. *Glob. Planet. Change* 64.
329 <https://doi.org/10.1016/j.gloplacha.2008.04.004>
- 330 10. Andrés-Anaya, P., Sánchez-Aparicio, M., del Pozo, S., Lagüela, S., 2021. Correlation of Land
331 Surface Temperature with IR Albedo for the Analysis of Urban Heat Island. *Eng. Proc.* 8, 9.
332 <https://doi.org/10.3390/engproc2021008009>
- 333 11. Lopez-Cabeza, V.P., Alzate-Gaviria, S., Diz-Mellado, E., Rivera-Gomez, C., Galan-Marin, C.,
334 2022. Albedo influence on the microclimate and thermal comfort of courtyards under
335 Mediterranean hot summer climate conditions. *Sustain. Cities Soc.* 81, 103872.
336 <https://doi.org/10.1016/j.scs.2022.103872>
- 337 12. Doughty, C.E., Loarie, S.R., Field, C.B., 2012. Theoretical Impact of Changing Albedo on
338 Precipitation at the Southernmost Boundary of the ITCZ in South America. *Earth Interact.* 16,
339 1–14. <https://doi.org/10.1175/2012EI422.1>
- 340 13. Prikryl, P., Rušín, V., 2023. Occurrence of heavy precipitation influenced by solar wind high-speed
341 streams through vertical atmospheric coupling. *Front. Astron. Space Sci.* 10.

- 342 14. Sawadogo, Y., Koala, S., Zerbo, J.L., 2022. Rainfall and Temperature Variations over Burkina
343 Faso: Possible Influence of Geomagnetic Activity, Solar Activity and Associated Energies from
344 1975 to 2020. *Atmospheric Clim. Sci.* 12, 603–612. <https://doi.org/10.4236/acs.2022.124034>
- 345 15. Feynman, J., & Ruzmaikin, A. (1999). Modulation of cosmic ray precipitation related to climate.
346 *Geophysical Research Letters*, 26(14), 2057–2060. <https://doi.org/10.1029/1999GL900326>
- 347 16. Carslaw, K. S., Harrison, R. G., & Kirkby, J. (2002). Cosmic Rays, Clouds, and Climate. *Science*,
348 298(5599), 1732–1737. <https://doi.org/10.1126/science.1076964>
- 349 17. Yeghikyan, A. (2020). The irreplaceable role of ubiquitous cosmic rays in the space chemistry :
350 From the origin of complex species in interstellar molecular clouds to the ozone depletion in the
351 atmospheres of Earth-like planets. *Communications of the Byurakan Astrophysical Observatory*,
352 37–54. <https://doi.org/10.52526/25792776-2020.67.1-37>
- 353 18. Allen, M.R., Ingram, W.J., 2002. Constraints on future changes in climate and the hydrologic cycle.
354 *Nature* 419, 224–232. <https://doi.org/10.1038/nature01092>
- 355 19. O’Gorman, P.A., Muller, C.J., 2010. How closely do changes in surface and column water vapor
356 follow Clausius–Clapeyron scaling in climate change simulations? *Environ. Res. Lett.* 5,
357 025207.
- 358 20. Bao, J., Sherwood, S.C., Alexander, L.V., Evans, J.P., 2017. Future increases in extreme
359 precipitation exceed observed scaling rates. *Nat. Clim. Change* 7, 128–132.
360 <https://doi.org/10.1038/nclimate3201>
- 361 21. Changnon, S.A., Kunkel, K.E., Reinke, B.C., 1996. Impacts and Responses to the 1995 Heat
362 Wave: A Call to Action. *Bull. Am. Meteorol. Soc.* 77, 1497–1506. [https://doi.org/10.1175/1520-0477\(1996\)077<1497:IARTTH>2.0.CO;2](https://doi.org/10.1175/1520-0477(1996)077<1497:IARTTH>2.0.CO;2)
- 364 22. Anderson, B.G., Bell, M.L., 2009. Weather-Related Mortality. *Epidemiol. Camb. Mass* 20, 205–
365 213. <https://doi.org/10.1097/EDE.0b013e318190ee08>
- 366 23. Kalkstein, L.S., Greene, S., Mills, D.M., Samenow, J., 2011. An evaluation of the progress in
367 reducing heat-related human mortality in major U.S. cities. *Nat. Hazards* 56, 113–129.
368 <https://doi.org/10.1007/s11069-010-9552-3>
- 369 24. Kalkstein, L.S., Sailor, D., Shickman, K., Sheridan, S., Vanos, J., 2013. Assessing the health
370 impacts of urban heat island reduction strategies in the District of Columbia. Rep. DDOE ID.
- 371 25. Vanos, J.K., Kalkstein, L.S., Sanford, T.J., 2015. Detecting synoptic warming trends across the US
372 Midwest and implications to human health and heat-related mortality. *Int. J. Climatol.* 35, 85–
373 96. <https://doi.org/10.1002/joc.3964>
- 374 26. McGugan, E.A., 2001. Hyperpyrexia in the emergency department. *Emerg. Med.* 13, 116–120.
375 <https://doi.org/10.1046/j.1442-2026.2001.00189.x>
- 376 27. Matsoukis, A., Kamoutsis, A., Bollas, A., Chronopoulou-Sereli, A., 2013. Biometeorological
377 Conditions in the Urban Park of Nea Smirni in the Greater Region of Athens, Greece During
378 Summer, in: Helmis, C.G., Nastos, P.T. (Eds.), *Advances in Meteorology, Climatology and*
379 *Atmospheric Physics*, Springer Atmospheric Sciences. Springer, Berlin, Heidelberg, pp. 217–
380 222. https://doi.org/10.1007/978-3-642-29172-2_31

- 381 28. Qiu, G., Li, H., Zhang, Q., Chen, W., Liang, X., Li, X., 2013. Effects of Evapotranspiration on
382 Mitigation of Urban Temperature by Vegetation and Urban Agriculture. *J. Integr. Agric.* 12,
383 1307–1315. [https://doi.org/10.1016/S2095-3119\(13\)60543-2](https://doi.org/10.1016/S2095-3119(13)60543-2)
- 384 29. Dickinson, R.E., Henderson-Sellers, A., 1988. Modelling tropical deforestation: A study of GCM
385 land-surface parametrizations. *Q. J. R. Meteorol. Soc.* 114, 439–462.
386 <https://doi.org/10.1002/qj.49711448009>
- 387 30. D’Almeida, C., Vörösmarty, C.J., Hurr, G.C., Marengo, J.A., Dingman, S.L., Keim, B.D., 2007. The
388 effects of deforestation on the hydrological cycle in Amazonia: a review on scale and
389 resolution. *Int. J. Climatol.* 27, 633–647. <https://doi.org/10.1002/joc.1475>
- 390 31. Ouyang, Z., Sciusco, P., Jiao, T., Feron, S., Lei, C., Li, F., John, R., Fan, P., Li, X., Williams, C.A.,
391 Chen, G., Wang, C., Chen, J., 2022. Albedo changes caused by future urbanization contribute
392 to global warming. *Nat. Commun.* 13, 3800. <https://doi.org/10.1038/s41467-022-31558-z>
- 393 32. Canadell, J.G., Raupach, M.R., 2008. Managing Forests for Climate Change Mitigation. *Science*
394 320, 1456–1457. <https://doi.org/10.1126/science.1155458>
- 395 33. Jin, M., Dickinson, R.E., Zhang, D., 2005. The Footprint of Urban Areas on Global Climate as
396 Characterized by MODIS. *J. Clim.* 18, 1551–1565. <https://doi.org/10.1175/JCLI3334.1>
- 397 34. Legrand, J., Simon, P., 1989. Solar cycle and geomagnetic activity: A review for geophysicists.
398 Part I. The contributions to geomagnetic activity. *Ann Geophys* 7, 565–578.
- 399 35. Zerbo, J.-L., Ouattara, F.M., Amory-Mazaudier, C., Legrand, J.-P., Richardson, J.D., 2013. Solar
400 Activity, Solar Wind and Geomagnetic Signatures. *Atmospheric Clim. Sci.* 3, 610.
401 <https://doi.org/10.4236/acs.2013.34063>
- 402 36. Kakad, B., Kakad, A., Ramesh, D.S., Lakhina, G.S., 2019. Diminishing activity of recent solar
403 cycles (22–24) and their impact on geospace. *J. Space Weather Space Clim.* 9, A1.
404 <https://doi.org/10.1051/swsc/2018048>
- 405 37. Somaïla, K., Yacouba, S., Louis, Z.J., 2022. Solar wind and geomagnetic activity during two
406 antagonist solar cycles: Comparative study between the solar cycles 23 and 24. *Int. J. Phys.*
407 *Sci.* 17, 57–66. <https://doi.org/10.5897/IJPS2022.4998>
- 408 38. Gonzalez, W.D., Tsurutani, B.T., Clúa de Gonzalez, A.L., 1999. Interplanetary origin of
409 geomagnetic storms. *Space Sci. Rev.* 88, 529–562. <https://doi.org/10.1023/A:1005160129098>
- 410 39. Tsurutani, B.T., Gonzalez, W.D., Gonzalez, A.L.C., Tang, F., Arballo, J.K., Okada, M., 1995.
411 Interplanetary origin of geomagnetic activity in the declining phase of the solar cycle. *J.*
412 *Geophys. Res. Space Phys.* 100, 21717–21733. <https://doi.org/10.1029/95JA01476>
- 413 40. Smith, E.J., Wolfe, J.H., 1976. Observations of interaction regions and corotating shocks between
414 one and five AU: Pioneers 10 and 11. *Geophys. Res. Lett.* 3, 137–140.
415 <https://doi.org/10.1029/GL003i003p00137>
- 416 41. Echer, E., Gonzalez, W.D., Alves, M.V., 2006. On the geomagnetic effects of solar wind
417 interplanetary magnetic structures. *Space Weather* 4. <https://doi.org/10.1029/2005SW000200>
- 418 42. Kopp, G., Lean, J.L., 2011. A new, lower value of total solar irradiance: Evidence and climate
419 significance. *Geophys. Res. Lett.* 38. <https://doi.org/10.1029/2010GL045777>
- 420 43. Bard, E., Frank, M., 2006. Climate change and solar variability: What’s new under the Sun. *epsl*

421 248, 1. <https://doi.org/10.1016/j.epsl.2006.06.016>

422 44. Lean, J., Rottman, Gary, Harder, J., Kopp, G., 2005. *SORCE Contributions to New Understanding*
423 *of Global Change and Solar Variability*, in: Rottman, G., Woods, T., George, V. (Eds.), *The*
424 *Solar Radiation and Climate Experiment (SORCE): Mission Description and Early Results*.
425 Springer, New York, NY, pp. 27–53. https://doi.org/10.1007/0-387-37625-9_3

426 45. Svensmark, H., 1998. Influence of Cosmic Rays on Earth's Climate. *Phys. Rev. Lett.* 81, 5027–
427 5030. <https://doi.org/10.1103/PhysRevLett.81.5027>

428 46. <https://power.larc.nasa.gov/data-access-viewer/>

429 47. <https://omniweb.gsfc.nasa.gov/form/dx1.html>

430 48. <http://www.sidc.be/silso/>

431